Available online at www.sciencedirect.com
SCIENCE DIRECT®
Journal of Molecular Catalysis A: Chemical 240 (2005) 7–15
JOURNAL OF MOLECULAR CATALYSIS A: CHEMICAL
www.elsevier.com/locate/molcata

Monomeric ruthenium carbonyls containing 2-substituted pyrazines From synthesis to catalytic activity in 1-hexene hydroformylation

M.A. Moreno, M. Haukka *, A. Turunen, T.A. Pakkanen

Department of Chemistry, University of Joensuu, P.O. Box 111, 80101 Joensuu, Finland

Received 11 May 2005; received in revised form 14 June 2005; accepted 15 June 2005
Available online 25 July 2005

Abstract

Synthesis and catalytic properties of a series of ruthenium carbonyl complexes with 2-substituted pyrazine ligands (pz–R; R = Cl, OMe, SMe, CN, NH_2) have been studied. Reactions between the $[Ru(CO)_3Cl_2]_2$ and the pyrazines led mainly to mononuclear compounds of the type $[Ru(CO)_3Cl_2(R–pz)]$. All of these ruthenium pyrazine compounds showed activity in 1-hexene hydroformylation. With an exception of NH_2, addition of the substituent to the pyrazine ring was found to improve the catalytic activity compared to the unsubstituted pyrazine. The catalytic cycle was studied by computational DFT methods. The results suggest that the key step in the formation of the active species involves release of one of the carbonyl in the *cis* position with respect to the pyrazine ring.

Keywords: Ruthenium; Pyrazines; Hydroformylation

1. Introduction

Ruthenium complexes containing pyrazine have been studied widely in recent decades because of their electrochemical and photochemical properties [1–4]. Dimeric pyrazine-bridged complexes in particular have been of interest due to the electron transfer, π-backbonding and delocalization phenomena [5–8]. All of these properties are strongly related to the character of the pyrazine ring, a highly delocalized electron system with two reactive sites. This feature makes pyrazine an intriguing ligand for the study of dinuclear or multinuclear mixed-valence [9–11] and mixed-metal complexes [12–13].

More recently, pyrazine-containing ruthenium complexes have found applications in the development of anti-metastatic drugs [14], as potential links to DNA [15], and as modulators of the immune response [16]. Catalytic applications of these complexes have been intermittently studied, including catalysts formed in situ for hydroformylation [17], and as catalysts for organic syntheses such as the hydroxylation of hydrocarbons [18].

In the current paper we report the synthesis and characterization of a series of ruthenium complexes containing monodentate 2-substituted pyrazine ligands. The catalytic activity is also tested for 1-hexene hydroformylation. The substituent effect on the reactivity of the pyrazine ligands and the ruthenium complexes is discussed and a catalytic cycle for the hydroformylation of 1-hexene is proposed based on spectroscopical evidence and computational DFT studies.

2. Experimental

FT-IR measurements were performed on a Nicolet Magna 750 spectrometer. ^{1}H NMR of the metallic complexes was recorded on a Bruker Avance with a resonance frequency of 250 MHz. Elemental analysis of the complexes was performed on EA1110 CHNS-O equipment (CE instruments). All of the reactions were performed under nitrogen and the solvents were also degassed prior to use. Crystals were obtained by recrystallization from a 1:1 mixture of hexane and dichloromethane.

* Corresponding author. Tel.: +358 13 251 3346; fax: +358 13 251 3344.
E-mail address: matti.haukka@joensuu.fi (M. Haukka).

1381-1169/$ – see front matter © 2005 Elsevier B.V. All rights reserved.
doi:10.1016/j.molcata.2005.06.028

2.1. General synthetic procedure

The complex $[Ru(CO)_3Cl_2(pz)]$ was obtained based on a solvent modification of the original synthesis by Dragonetti et al. [19] using ethanol instead of dichloromethane. The complexes $[Ru(CO)_3Cl_2(2\text{-}Cl\text{–}pz)]$ (**1**), $[Ru(CO)_3Cl_2(2\text{-}CN\text{–}pz)]$ (**2**), $[Ru(CO)_3Cl_2$ (2-OMe–pz)] (**3**), $[Ru(CO)_3Cl_2(2\text{-}SMe\text{–}pz)]$ (**4**), $[Ru(CO)_2Cl_2(2\text{-}NH_2\text{–}pz)_2(COOCH_2CH_3)]$ (5) and $[Ru(CO)_2Cl_2(2\text{-}NH_2\text{–}pz)_2]$ (**6**) were prepared in ethanol as follows: 200 mg (0.391 mmol) of $[Ru(CO)_3Cl_2]_2$ and 228 mg of the pyrazine (2.314, 2.559, 2.423, 2.070 and 2.882 mmol of 2-chloropyrazine, 2-carbonitrilepyrazine, 2-methoxypyrazine, 2-thiomethylpyrazine, and 2-aminopyrazine, respectively) were dissolved in separated flasks in 4 ml of degassed ethanol. The solutions were combined and stirred overnight (17 h). A solid precipitate was filtered, washed with ethanol and dried under vacuum:

$$[Ru(CO)_3Cl_2(2\text{-}Cl\text{–}pz)] \quad (1)$$

2-Cl–pz = 2-chloropyrazine. ν(CO) = 2058, 2082, 2141 cm^- in CH_2Cl_2, δ_H(DMSO) 8.5d; 8.6d. Anal. Calc.% C: 22.69% N: 7.56% H: 0.82. Found % C: 22.71% N: 7.42% H: 0.91. Yield = 92%:

$$[Ru(CO)_3Cl_2(2\text{-}CN\text{–}pz)] \quad (2)$$

2-CN–pz = 2-carbonitrilepyrazine. ν(CO) = 2060, 2084, 2142 cm^{-1} in CH_2Cl_2, δ_H(DMSO) 8.8d; 8.9d. Anal. Calc.% C: 26.61% N: 11.64% H: 0.84. Found% C: 26.79% N: 11.41% H: 0.96. Yield = 89%:

$$[Ru(CO)_3Cl_2(2\text{-}OMe\text{–}pz)] \quad (3)$$

2-OMe–pz = 2-methoxypyrazine. ν(CO) = 2059, 2077, 2139 cm^{-1} in CH_2Cl_2, δ_H(DMSO) 8.5s; 8.6d. Anal. Calc% C: 26.24% N: 7.65% H: 1.65. Found% C: 26.22% N: 7.54% H: 1.67. The solid precipitated at 4 °C. Yield = 78%:

$$[Ru(CO)_3Cl_2(2\text{-}SMe\text{–}pz)] \quad (4)$$

2-SMe–pz = 2-thiomethylpyrazine. ν(CO) = 2055, 2079, 2138 cm^{-1} in CH_2Cl_2, δ_H(DMSO) 8.7d; 8.8d. Anal. Calc.% C: 25,14% N: 7.33% H: 1.58. Found% C: 25.17% N: 7.27% H: 1.65. Yield = 80%:

$$[Ru(CO)_2Cl(2\text{-}NH_2\text{–}pz)_2(COOCH_2CH_3)] \quad (5)$$

2-NH_2–pz = 2-aminopyrazine. ν(CO) = 1623, 1994, 2065 cm^{-1} in KBr pellets, δ_H(DMSO); 7.9d; 8.3d Anal. Calc% C: 23.94% N: 11.97% H: 1.44. Found% C: 23.22% N: 11.54% H: 1.67. Yield = 62%:

$$[Ru(CO)_2Cl_2(2\text{-}NH_2\text{–}pz)_2] \quad (6)$$

2-NH_2–pz = 2-aminopyrazine. ν(CO) = 2001, 2066 cm^{-1} in KBr pellets, δ_H(DMSO) 8.3d; 8.4d Anal. Calc.% C: 29.72% N: 20.10% H: 2.41. Found% C: 29.22% N: 19.09% H: 2.61. This reaction was performed in dichloromethane. Yield = 82%:

$$[Ru(CO)_3Cl_2(2\text{-}NH_2\text{–}pz)] \quad (7)$$

$[RuCl_2(CO)_3(2\text{-}NH_2\text{–}pz)]$ was obtained by refluxing **(6)** with 200 mg (0.391 mmol) $[Ru(CO)_3Cl_2]_2$ in acetonitrile for 18 h, the ratio Ru/(5) was 2:1, a yellow product forms during evaporation of the solution. ν(CO) = 2065, 2082, 2141 cm^{-1} in CH_2Cl_2. δ_H(DMSO) 8.4d; 8.5d. Anal. Calc.% C: 23.94% N: 11.96% H: 1.43. Found% C: 23.91% N: 11.95% H: 1.33. Yield = 54%:

$$[Ru(CO)_3Cl_2(CH_3CN)] \quad (8)$$

Two hundred milligrams (0.391 mmol) of $[Ru(CO)_3Cl_2]_2$ were refluxed in acetonitrile for 8 h, the solvent was evaporated and the product was washed with dichloromethane. ν(CO) = 2066, 2083, 2141 cm^{-1} in CH_2Cl_2. $\delta_H(CDCl_3)$ 2.82s. Anal. Calc.% C: 20.22% N: 4.72% H: 1.02. Found% C: 20.11% N: 4.71% H: 1.18%. Yield = 75%:

2.2. Catalysis

The hydroformylation reactions were performed in high-pressure autoclaves (100 ml Berghof) equipped with a teflon liner. The autoclaves were charged in a glove box under nitrogen atmosphere. In a typical experiment, the solvent 1-methyl-2-pyrrolidinone (5 ml), the standard cyclohexane (0.2 ml), the olefin 1-hexene (0.5 ml), and the catalyst were added to the autoclave, which was then pressurized to 20 bar with synthesis gas CO/H_2 1:1. The autoclave was heated at 120 °C for 17 h. The reaction was then stopped and the autoclave was rapidly cooled to room temperature and brought to atmospheric pressure, after which the liquid samples were analysed. The product distribution is reported as weight%.

The gases CO and H_2 used in the hydroformylation experiments were of 99 and 99.99% purity, respectively. The solvent 1-methyl-2-pyrrolidinone (Aldrich 99%) and the internal standard cyclohexane (Merck 99%) were used without further purification and degassed with nitrogen before use. Similarly, 1-hexene (99%) was degassed prior to use. Gas chromatographic analyses of the product mixture were recorded on a Hewlett-Packard 5890 series II chromatograph equipped with a Varian WCOT fused silica 50 M × 0.53 M column and temperature programming

2.3. X-ray structure determinations

Crystals were immersed in cryo-oil, mounted in a Nylon loop and measured at a temperature of 120 or 150 K. The X-ray diffraction data was collected by means of a Nonius KappaCCD diffractometer using Mo Kα radiation (λ = 0.71073 Å). The Denzo-Scalepack [20] program package was used for cell refinements and data reduction. The structures were solved by direct methods using the SIR2000 program. [21] A multiscan absorption correction based on equivalent reflections (XPREP in SHELXTL v.

Table 1
Crystal Data for Compounds 1–4

sa	1	2	3	4
Empirical formula	$C_7H_3Cl_3N_2O_3Ru$	$C_8H_3Cl_2N_3O_3Ru$	$C_8H_6Cl_2N_2O_4Ru$	$C_8H_6Cl_2N_2O_3RuS$
fw	370.53	361.10	366.12	382.18
Temp (K)	120(2)	120(2)	120(2)	120(2)
λ(Å)	0.71073	0.71073	0.71073	0.71073
Cryst syst	Tetragonal	Orthorhombic	Monoclinic	Monoclinic
Space group	$I\bar{4}$	$P2_12_12_1$	$P2_{1/c}$	$P2_{1/c}$
a (Å)	19.513(2)	5.77300(10)	6.97100(10)	10.7458(3)
b (Å)	19.513(2)	13.5063(4)	11.9620(2)	10.6744(6)
C (Å)	6.1269(7)	15.0242(6)	15.2290(3)	11.2329(9)
β (deg)	90	90	102.7550(10)	94.280(3)
V (Å^3)	2332.9(5)	1171.46(6)	1238.56(4)	1284.88(13)
Z	8	4	4	4
ρ_{calc} (Mg/m^3)	2.110	2.047	1.963	1.976
μ (Mo Kα) (mm^{-1})	2.021	1.791	1.699	1.793
R1[a] ($I \geq 2\sigma$)	0.0488	0.0254	0.0195	0.0365
wR2[b] ($I \geq 2\sigma$)	0.1077	0.0544	0.0439	0.0681

Table 2
Selected bond lengths (Å) and angles (deg) for 1–4

as	1	2	3	4
Ru(1)–Cl(2)	2.401(3)	2.4008(7)	2.3963(4)	2.3993(9)
Ru(1)–Cl(3)	2.401(2)	2.3972(8)	2.3942(4)	2.4012(8)
Ru(1)–C(1)	1.910(12)	1.928(4)	1.9235(19)	1.932(4)
Ru(1)–C(2)	1.946(13)	1.907(3)	1.9162(19)	1.917(4)
Ru(1)–C(3)	1.919(13)	1.921(4)	1.9099(19)	1.909(4)
Ru(1)–N(1)	2.140(8)	2.132(3)	2.1453(14)	2.148(3)
C(1)–Ru(1)–N(1)	174.9(4)	173.13(13)	174.46(7)	175.26(12)
C(2)–Ru(1)–Cl(2)	179.5(3)	178.59(10)	176.21(5)	176.63(9)
C(3)–Ru(2)–Cl(3)	176.8(3)	176.95(10)	178.20(5)	177.50(9)

6.12) [22] was applied to all of the data (the T_{min}/T_{max} values were 0.6637/0.9092, 0.6283/0.8525, 0.4868/0.6386, 0.7503/0.8954 for **1–4**, respectively). Structural refinements were carried out using SHELXL-97 with the WinGX graphical user interface [23–24]. All of the hydrogens were placed in idealized positions and constrained to ride on their parent atom. The crystallographic data is summarized in Table 1 and the selected bond lengths and angles in Table 2. The thermal ellipsoid plots of **1–4** with the numbering schemes are shown in Figs. 1–4.

2.4. Computational details

The geometries of the complexes were optimised using the B3PW91 hybrid density functional method and employing 6–31G* as a basis set (for ruthenium: Huzinaga's extra basis 433321/4331/421) [25]. The geometry optimisations were followed by analytical frequency calculations to obtain the vibration spectra and the stationary point of all compounds. The calculations were carried out using Gaussian-03 program. The proton affinities of the ligands were also calculated. The basis set superposition error (BSSE) correction was estimated from a single point calculation by adding ghost functions in place of hydrogen in the optimised protonated structures.

3. Results and discussion

3.1. Reaction studies

Reactions between the ruthenium dimer and the selected pyrazines yielded mainly mononuclear ruthenium compounds of the type [Ru(CO)$_3$Cl$_2$(2-pz)] (see Figs. 1–4). In the case of unsubstituted pyrazine, the formation of a dimer as a secondary product [19] was observed. The substituent

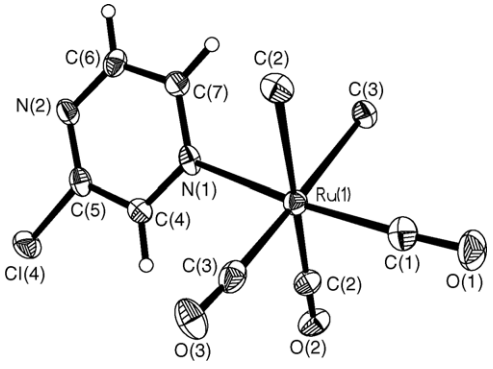

Fig. 1. Thermal ellipsoid view of complex [Ru(CO)$_3$Cl$_2$(2-Cl–pz)] (1) with the atomic numbering scheme. The thermal ellipsoids are drawn with 50% probability.

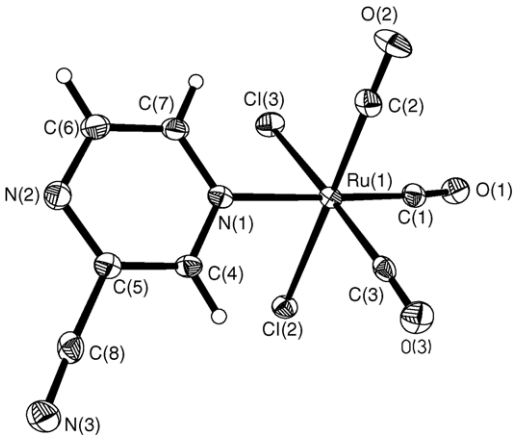

Fig. 2. Thermal ellipsoid view of complex $[Ru(CO)_3Cl_2(2\text{-CN–pz})]$ (2) with the atomic numbering scheme. The thermal ellipsoids are drawn with 50% probability.

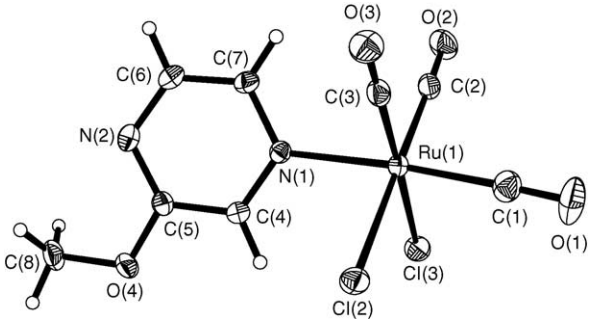

Fig. 3. Thermal ellipsoid view of complex $[Ru(CO)_3Cl_2(2\text{-OMe–pz})]$ (3) with the atomic numbering scheme. The thermal ellipsoids are drawn with 50% probability.

probably makes the second nitrogen less eager to bind to another metal center, thus reducing the tendency to obtain bridged Ru–pz–Ru complexes.

In general, most of the substituted pyrazines behaved quite similarly. However, aminopyrazine followed somewhat different reaction routes depending on the solvent. In ethanol an alkoxycarbonyl complex of $[Ru(CO)_2Cl(2\text{-}NH_2\text{–pz})_2(COOCH_2CH_3)]$ (**5**) was obtained, while use of dichloromethane led to a mononuclear bis-pz compound of $[Ru(CO)_2Cl_2(2\text{-}NH_2\text{–pz})_2]$ (**6**). Formation of the mono pyrazine $[Ru(CO)_3Cl_2(2\text{-}NH_2\text{–pz})]$ (**7**), which was the dominating type of product with the other pyrazines in ethanol

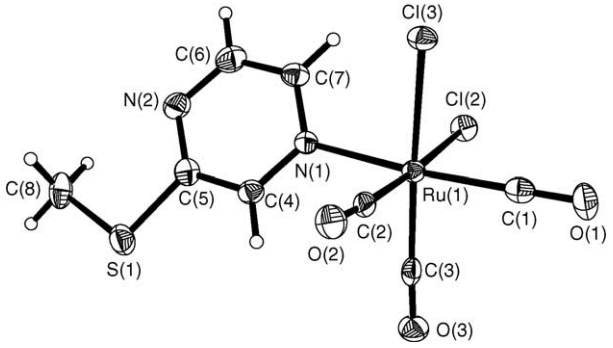

Fig. 4. Thermal ellipsoid view of complex $[Ru(CO)_3Cl_2(2\text{-SMe–pz})]$ (4) with the atomic numbering scheme. The thermal ellipsoids are drawn with 50% probability.

reactions, was observed only when the bis-complex (**5**) was allow to react further with additional $[Ru(CO)_3Cl_2]_2$ in acetonitrile.

In order to determine the effect of the substituent on the pyrazine ring, the reactivity of the different pz ligands and the complex formation was studied further by using DFT methods. The general chemical behavior of the pyrazine ligands was estimated by calculating the proton affinities.

The geometries of the computationally optimised isolated ruthenium complexes were in good agreement with the experimental crystal structures, and no significant deviations were observed. Formation enthalpies were calculated by modeling the reactions shown in Eqs. (1), (2) and (3). The results are summarized in Table 3:

$$[Ru(CO)_3Cl_2]_2 + 2\,(2\text{-x–pz}) \rightarrow 2\,[Ru(CO)_3Cl_2(2\text{-x–pz})] \quad (1)$$

(2-x = 2-Cl, 2-CN, 2-OMe, 2-SMe, pz = pyrazine)

$$[Ru(CO)_3Cl_2]_2 + 4\,(2\text{-y–pz}) \rightarrow 2\,[Ru(CO)_2Cl_2(2\text{-y–pz})_2] \quad (2)$$

$$[Ru(CO)_3Cl_2]_2 + 4\,(2\text{-y–pz}) + EtOH \rightarrow 2\,[Ru(CO)_2Cl(2\text{-y–pz})_2(COOEt)] + 2HCl\ 2\text{-y} = 2\text{-}NH_2 \quad pz = pyrazine \quad (3)$$

All of the reactions were thermodynamically favored. The differences in energy values can be attributed to the effect of the substituent in the pyrazine ligand. The results indicate

Table 3
Calculated temperature-corrected formation enthalpies for the complexes

Reaction	ΔH kJ/mol
$[Ru(CO)_3Cl_2]_2 + 2\ (2\text{-CN–pz}) \rightarrow 2[Ru(CO)_3Cl_2(2\text{-CN–pz})]$	−24.52
$[Ru(CO)_3Cl_2]_2 + 2\ (2\text{-Cl–pz}) \rightarrow 2[Ru(CO)_3Cl_2(2\text{-Cl–pz})]$	−33.78
$[Ru(CO)_3Cl_2]_2 + 2\ (pz) \rightarrow 2[Ru(CO)_3Cl_2(pz)]$	−52.50
$[Ru(CO)_3Cl_2]_2 + 2\ (2\text{-OMe–pz}) \rightarrow 2[Ru(CO)_3Cl_2(2\text{-OMe–pz})]$	−56.77
$[Ru(CO)_3Cl_2]_2 + 2\ (2\text{-SMe–pz}) \rightarrow 2[Ru(CO)_3Cl_2(2\text{-SMe–pz})]$	−55.18
$[Ru(CO)_3Cl_2]_2 + 2\ (2\text{-}NH_2\text{–pz}) \rightarrow 2[Ru(CO)_3Cl_2(2\text{-}NH_2\text{–pz})]$	−61.70
$[Ru(CO)_3Cl_2]_2 + 4\ (2\text{-}NH_2\text{–pz}) \rightarrow 2[Ru(CO)_2Cl_2(2\text{-}NH_2\text{–pz})_2] + 2CO$	−37.94
$[Ru(CO)_3Cl_2] + 4(2\text{-}NH_2\text{–pz}) + EtOH \rightarrow 2[Ru(CO)_2Cl(2\text{-}NH_2\text{–pz})_2(COOEt)] + HCl$	−11.21

Table 4
Calculated proton affinities for the free ligands

Ligand	Proton affinity kJ/mol
2-NH_2–pz	925.5
2-OMe–pz	910.0
2-SMe–pz	906.8
pz	883.1/887.7[a]
2-Cl–pz	860.4
2-CN–pz	831.5

[a] Experimental value [28].

that those mono-pyrazine complexes that contain electron-donating groups in the pyrazine ring are energetically more favored than those containing electron-withdrawing groups. Although the formation enthalpy for the complex $[Ru(CO)_3Cl_2(2\text{-}NH_2\text{–}pz)]$ is highly favorable, this complex cannot be obtained following the same synthetic procedure as the rest of the pyrazine complexes, but instead the complex $[Ru(CO)_2Cl(2\text{-}NH_2\text{–}pz)_2(COOEt)]$ is formed. This is probably due to the high reactivity of the aminopyrazine ligand towards the alcohol solvent favoring the formation of nucleophilic alkoxy groups. This type of reaction of the aromatic nitrogen ligand has been observed previously in reactions between bipyridines and $[Ru(CO)_3Cl_2]_2$ [26,27]. To avoid the formation of alkoxy carbonyl, the solvent was changed to dichloromethane and the product obtained was the bis pyrazine complex $[Ru(CO)_2Cl_2(2\text{-}NH_2\text{–}pz)_2]$. This is again due to the higher reactivity of the 2-NH_2–pz, which makes it capable of replacing a carbonyl in the ruthenium center.

In order to study in detail the differences in the properties of the substituted pyrazines, we estimated the degree of reactivity of these ligands towards protons by calculating the proton affinities. The results are summarized in Table 4.

The trend of proton affinity values is as follows: 2-NH_2–pz > 2-OMe–pz > 2-SMe–pz > pz > 2-Cl–pz > 2-CN–pz. This shows that the ligand 2-NH_2–pz has the highest value. The high proton affinity can facilitate a nucleophilic attack in an alcohol solution by favoring the formation of alkoxy groups, and subsequently the formation of a $[Ru(CO)_2Cl_2(2\text{-}NH_2\text{–}pz)(COOEt)]$ type of complexes. The reaction of $[Ru(CO)_3Cl_2]_2$ with bipyridines in alcohols is known to lead to alkoxycarbonyls $[Ru(CO)_2Cl(bpy)(COOR)]$ [28], while the proton affinity of the bipyridine is higher than the corresponding value of any of the pyrazines studied [29].

The proton affinities in Table 4 are also in agreement with the values of the ruthenium complex formation enthalpies (Table 3), which suggest that in the case of pyrazines the proton affinity could also reflect more general reactivity trend of these ligands. In other words, the more reactive is the ligand the more favored is the reaction.

3.2. Catalytic studies

All ruthenium pyrazine complexes were tested as catalysts for the hydroformylation of 1-hexene. The results are summarized in Table 5.

Table 5
Catalytic activity for the hydroformylation of 1-hexene

Catalyst	Yield[a] (%)	1-Hexene (%)	Isomers (%)	2-Et-pentanal (%)	2-Me-hexanal (%)	1-Heptanal (%)	Total Aldehydes (%)	*n:i* ratio (%)	2-Et-pentanol (%)	2-Me-hexanol (%)	1-Heptanol (%)	Total Alcohols (%)	*n:i* ratio
$[Ru(CO)_3Cl_2(pz)]$	31	46	23	–	9	10	19	1.2	–	4	8	12	1.7
$[Ru(CO)_3Cl_2$ (2-OMe–pz)] (**3**)	66	10	24	6	15	24	45	1.2	4	3	14	21	1.9
$[Ru(CO)_3Cl_2$ (2-SMe–pz)] (**4**)	48	30	23	5	11	15	31	0.9	3	3	11	17	1.8
$[Ru(CO)_3Cl_2$ (2-CN–pz)] (**2**)	35	47	18	4	9	16	30	1.0	–	–	5	5	–
$[Ru(CO)_3Cl_2$ (2-Cl–pz)] (**1**)	72	21	7	5	12	16	32	0.8	6	8	26	40	1.8
$[Ru(CO)_3Cl_2$ (2-NH_2–pz)] (**7**)	26	66	8	–	9	13	22	1.4	–	–	4	4	–
$Ru(CO)_3Cl_2(CH_3CN)]$ (**8**)	80	6	8	7	16	23	50	0.9	3	7	18	28	1.8
$[Ru(CO)_3Cl_2]_2$	82	8	10	9	18	25	52	0.9	4	7	19	30	1.7

Conditions: T = 120 °C; react time = 17 h; n(Ru) = 0.08 mmol; V(solvent) = 5 ml 1-methyl-2-pyrrolidinone; V(1-hexene) = 0.5 ml; V(standard) = 0.2 ml cyclohexane; P CO/H_2 1:1 20 bar.
[a] Yield% = hydroformylation products, % aldehydes + % alcohol.

The catalytic activities of any substituted-pyrazine complexes were found to be higher than the activity of plain pyrazine, except for the aminopyrazine complex. The two other 2-NH_2–pz complexes $[Ru(CO)_2Cl_2(2\text{-}NH_2\text{–}pz)_2]$ and $[Ru(CO)_2Cl(2\text{-}NH_2\text{–}pz)_2(COOCH_2CH_3)]$, were also tested, but in these cases the low solubility in 1-methyl-2-pyrrolidinone (solvent employed for the catalytic runs) prevent the catalytic reaction completely. The trend in total catalytic activity (total conversion) follows the order of Ru–(2-Cl–pz) > Ru–(2-OMe–pz) > Ru–(2-SMe–pz) > Ru–(2-CN–pz) > Ru–(pz) > Ru–(2-NH_2–pz). All of the complexes produce both aldehydes and alcohols showing hydroformylation is followed by the hydrogenation of aldehydes. Product distribution was confirmed by quantitative ^{13}C NMR and no evidence of hexane formation was found, suggesting that unlike the aldehydes, the substrate does not undergo hydrogenation. Alcohols are not a rare product in ruthenium catalysed hydroformylation [30–32] and ruthenium complexes have been reported to be good hydrogenation catalysts [33–35]. In the coordinated complexes, the activity pattern does not follow the order of the simple electron-donating/electron-withdrawing effects induced by the substituent. Similar activities were observed for complexes with strong electron donor group in the pyrazine ring and for complexes with electron-withdrawing groups. This suggests that the electron-donating/electron-withdrawing effect of the substituent does not play the determining role in the overall activity of the metal complex.

The main reason behind the poor activity displayed by the unsubstituted pyrazine complex is its tendency to produce a dimeric-bridged Ru–pz–Ru complex [19], which, is catalytically more stable and consequently less reactive [36]. With any other pyrazine the presence of a substituent hinders the formation of dimers. In addition to possible steric effects, the substituent (in ortho position with the non-coordinated nitrogen) has a deactivating effect on the remaining nitrogen. This may be due to a decrease in the basicity of the coordinated pyrazines. Such an effect has been reported in the literature based on backbonding effects [37].

The possible catalytic routes for alkene hydroformylation based on computational and spectroscopic results are shown in Scheme 1. Evidence of catalyst regeneration was observed

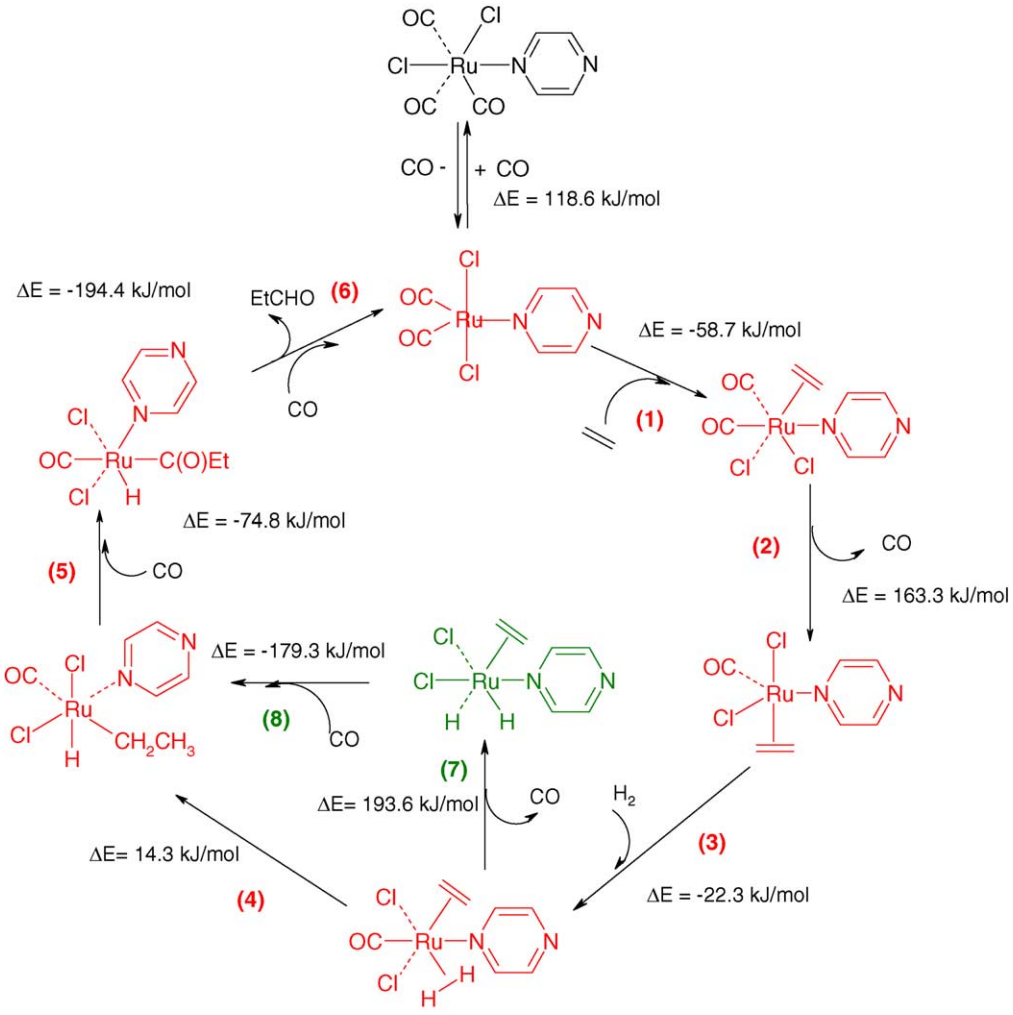

Scheme 1. Possible routes for the hydroformylation of ethylene by $[Ru(CO)_3Cl_2(pz)]$ Et = CH_2CH_3.

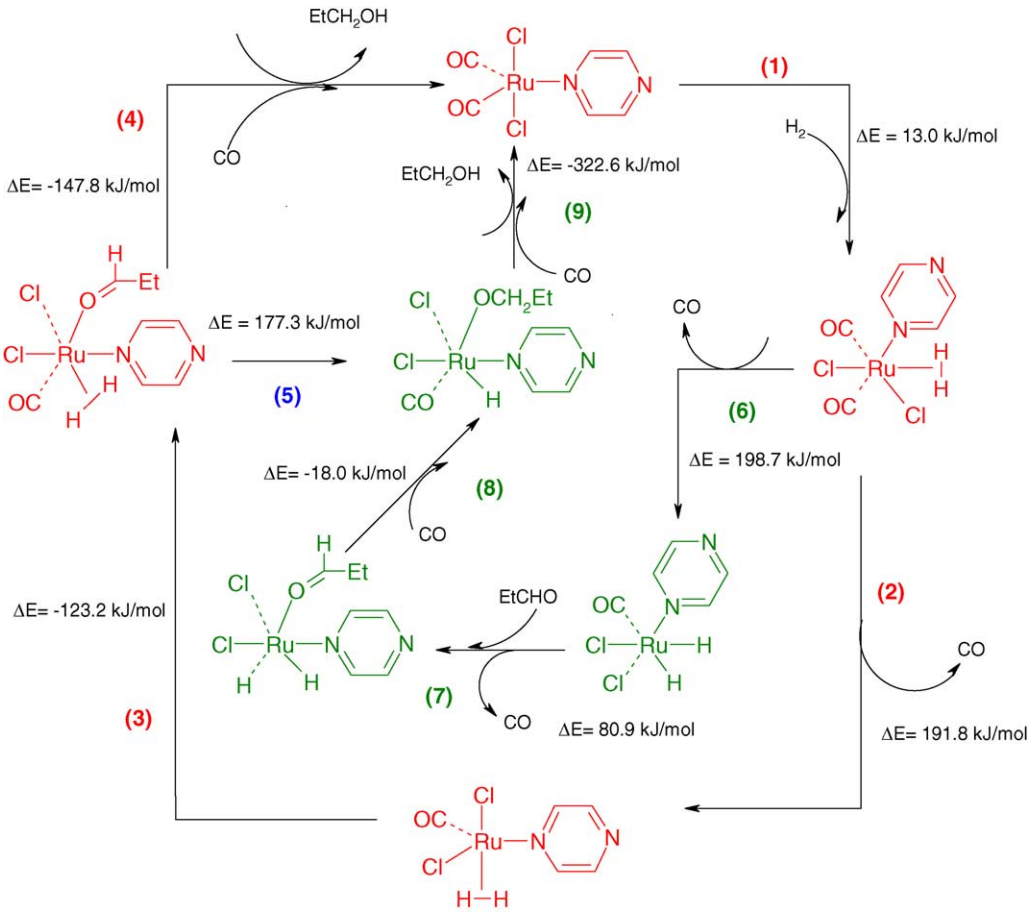

Scheme 2. Possible routes for the hydrogenation of propanal by $[Ru(CO)_3Cl_2(pz)]$, Et = CH_2CH_3.

by means of FT-IR and NMR analyses of the solid recovered after catalysis. Since all ruthenium pyrazine complexes produce both aldehydes and alcohols, we also discussed the possible catalytic routes for the hydrogenation of aldehydes in Scheme 2.

The routes were modeled computationally in gas phase using ethylene instead of 1-hexene as the starting alkene in order to simplify the system geometrically. In both hydroformylation and hydrogenation the initiation step involves the loss of carbonyl. The release of carbonyl from the initial ruthenium complex is rather plausible. Furthermore, experimental evidence of such a release was observed by means of FT-IR. A suspension of the complex $[Ru(CO)_3Cl_2(pz)]$ in 1-hexene was placed in an autoclave and heated at 120 °C for 17 h (catalytic conditions). A gas sample was taken after the reaction, revealing carbon monoxide in the gas phase. The liquid phase showed a mixture of tricarbonyl (νCO = 2061 s, 2080 s (broad), 2136 m cm^{-1} in CH_2Cl_2) and dicarbonyl (νCO = 2016 s, 2080 s (broad) cm^{-1} in CH_2Cl_2). ^{1}H NMR analysis of the solid recovered showed signals at δ_H(DMSO) 8.9dd (J = 15.2 Hz), and 9.06dd (J = 12.3 Hz) confirming that pyrazine was still coordinated to the metal. The complex $[Ru(CO)_3Cl_2(pz)]$ is also able to release carbonyl at room temperature in acetonitrile, confirming the facile decarbonylation process.

According to our results, the initial vacancy is generated via decarbonylation. Since the complex contains two types of carbonyl ligands, we estimated computationally the energy requirements for the release of both the *cis* and the *trans* carbonyls. In principle, the initial vacancy could also be generated via the release of pyrazine, which was also estimated. The results are presented in Table 6.

In all of the cases the release of *cis* carbonyl is energetically less demanding than the correspondent *trans* carbonyl or the pyrazine ligand. The presence of a substituent in the pyrazine complex probably plays a role in stabilizing the intermediates during the catalytic process, since the activities vary from one complex to another. Indirect evidence of the permanence of the pyrazine ring in the complex was observed when the reaction was performed using the ruthenium dimer alone (see Table 5). The activities observed were considerably higher. Thus, if pyrazine is released, the activities and selectivities should be comparable to those obtained with $[Ru(CO)_3Cl_2]_2$. This dimer is known to break in the presence of coordinating solvents generating units of $[Ru(CO)_3Cl_2(solv)]$ (see for example complex **8**) that are able to exchange easily the sol-

Table 6
Estimated required energies for the generation of the initial active site in the catalytic cycle

Complex	Release of *cis*-CO kJ/mol	Release of *trans*-CO kJ/mol	Release of pyrazine kJ/mol
$[Ru(CO)_3Cl_2$ (2-NH_2–pz)] (**7**)	118.59	158.75	135.73
$[Ru(CO)_3Cl_2$ (2-OMe–pz)] (**3**)	118.63	165.20	132.46
$[Ru(CO)_3Cl_2$ (2-SMe–pz)] (**4**)	121.28	163.86	133.26
$[Ru(CO)_3Cl_2$(pz)]	118.59	166.25	131.28
$[Ru(CO)_3Cl_2$ (2-Cl–pz)] (**1**)	118.36	169.32	129.77
$[Ru(CO)_3Cl_2$ (2-CN–pz)] (**2**)	118.67	171.54	121.14
$[Ru(CO)_3Cl_2$ (CH_3CN)] (**8**)	122.61	173.44	108.21 CH_3CN[a]

[a] CH_3CN: refers to the loss of acetonitrile in complex (**8**).

vent molecule [38,39]. In this case the solvent intermediate provides a good active species in which the solvent can be exchanged by the alkene substrate. This is in agreement with the catalytic activity exhibited by the acetonitrile complex $[Ru(CO)_3Cl_2(CH_3CN)]$ (8). It's activity is comparable to the dimer $[Ru(CO)_3Cl_2]_2$, unlike any of the pyrazine-containing complexes. This constitutes indirect evidence of the permanence of the pyrazine ligand in the catalyst. Moreover, the energy required for the release of acetonitrile from complex 8 is lower than the energy necessary to release carbonyl (see Table 6). This imply that the mechanism of activation for the pyrazine complexes goes through a different path respect to the dimer $[Ru(CO)_3Cl_2]_2$ or the acetonitrile complex $[Ru(CO)_3Cl_2(CH_3CN)]$ who seem to follow the same mechanism.

In the proposed hydroformylation cycle (steps 1–6, in Scheme 1) a pentacoordinated ruthenium complex coordinates alkene (step 1). The next step involves decarbonylation to create a vacancy for dihydrogen to coordinate (step 2). During the step 3 hydrogen fill the vacancy producing the dihydrogen intermediate ruthenium dihydrogen complexes have been previously reported in the literature [40–43] and metal-dihydrogen species are proposed to be active intermediates in several hydrogenation reactions [44–46]. The next step involves the intramolecular transfer of hyrdogen to the alkene [47] to form the $Ru(H)(CH_2CH_3)$ intermediate (step 4). This type of mechanism of stepwise hydrogen transfer has been proposed by Lau and Cheng for hydrogenation of alkenes [46]. Carbonyl insertion is the next step (step 5), followed by the generation of the aldehyde unit (step 6). An alternative route (steps 1–3, 7–8 and 5–6) involves the formation of a metal dihydride intermediate instead of intramolecular hydrogen transfer (step 7). Although the hydrogenation of the alkene from the dihydride complex is higly favorable (step 8), the formation of dihydride is not (step 7).

In principle, the hydrogenation of the aldehyde can take place in three different ways shown in Scheme 2. The initial active complex of dicarbonyl dichloride ruthenium pyrazine coordinates hydrogen in the form of a dihydrogen unit (step 1, in Scheme 2). In the next step another carbonyl is released to generate a vacancy for coordination of the aldehyde (step 2). Step 3 comprises the formation of the $Ru(H_2)(OCH_2Et)$ intermediate. Ruthenium intermediates of this type have been proposed previously in the literature [48]. In the final step (4) the aldehyde is hydrogenated via simultaneous hydrogen transfer in a mechanism that has been proposed by Poliakoff in his studies on metal carbonyl dihydrogen complexes in hydrogenation, [49] producing alcohol and regenerating the initial active complex. The alternative mechanism involves the formation of a dihydride intermediate (step 6). The next step involves then coordination of the aldehyde via decarbonylation (step 7). This is followed by the hydrogenation of the carbonyl double bond producing the alkoxy intermediate (step 8). Finally, alcohol is released allowing CO to coordinate and regenerate the active complex (step 9). The third possible mechanism involves again steps 1–3, but instead of simultaneous hydrogen transfer, it involves stepwise mechanism producing an alkoxy complex from the dihydrogen intermediate (step 5). By comparing the total energy differences for each hydrogenation mechanism it was found that simultaneous hydrogen transfer ($\Delta E_{tot} = -66.2$ kJ/mol) and stepwise hydrogen transfer ($\Delta E_{tot} = -63.7$ kJ/mol) mechanisms are more favorable than hydrogenation via dihydride intermediates ($\Delta E_{tot} = -47.9$ kJ/mol). According to these results the first two mechanisms are the most plausible ones.

4. Conclusions

The reactivity of the substituted pyrazine ligands is closely related to the type of substituent in the ring and to their intrinsic electronic properties. Thus, a strong electron donor in the ring increases the reactivity of the ligand, while electron-withdrawing groups produce the opposite effect. The ligand aminopyrazine is particularly sensitive to the reaction conditions employed during synthesis, producing bis-pyrazine and alkoxycarbonyl complexes in which the direct participation of the solvent in the reaction is present. This is an advantage in terms of tailoring and designing new synthetic routes.

Substitution of the pz ligand improves the catalytic activity of ruthenium complexes. This is mainly due to the reduced tendency of the $[Ru(CO)_3Cl_2$(2-pz)] complexes to form catalytically less active dimers of the type Ru–pz–Ru. According to the DFT results and spectroscopic evidence, the activation of the ruthenium pyrazine complexes in hydroformylation is initiated by the release of the carbonyl-positioned *cis* to the pyrazine ligand.

The activation of the ruthenium dimer $[Ru(CO)_3Cl_2]_2$ and the acetonitrile complex $[Ru(CO)_3Cl_2(CH_3CN)]$ proceeds in a different way respect to the pyrazine-containing complexes. The complexes activates by exchanging the solvent molecule instead of releasing carbonyl.

Acknowledgement

Financial support provided by the Academy of Finland and COST D29 is gratefully acknowledged (M.H.).

Appendix A. Supplementary information

CCDC-271424 (**1**), CCDC-271425 (**2**), CCDC-271426 (**3**), CCDC-271427 (**4**) contains the supplementary crystallographic data for this paper. These data can be obtained free of charge from The Cambridge Crystallographic Data Centre via www.ccdc.cam.ac.uk/data_request/cif.

References

[1] R. Hage, H.E.B. Lempers, J.G. Haasnoot, J. Reedijk, F.M. Weldon, J.G. Vos, Inorg. Chem. 36 (14) (1997) 3139–3145.
[2] P.A. Lay, R.H. Mangunson, H. Taube, Inorg. Chem. 27 (13) (1988) 2364–2371.
[3] R. De la Rosa, P.J. Chang, F. Salaymeh, J.C. Curtis, Inorg. Chem. 24 (25) (1985) 4229–4231.
[4] G. Di Marco, A. Bartolotta, V. Ricevutto, S. Campagna, G. Denti, L. Sabatino, G. De Rosa, Inorg. Chem. 30 (2) (1991) 270–275.
[5] D. Brown, S. Muranjan, R.P. Thummel, Eur. J. Inorg. Chem. 19 (2003) 3547–3553.
[6] H. Casey, C.P. Kubiack, J. Phys. Chem. A. 107 (44) (2003) 9301–9311.
[7] L.T. Zhang, M.J. Ondrechen, Inorg. Chim. Acta 226 (1–2) (1994) 43–51.
[8] T. Yamaguchi, N. Imai, T. Ito, C.P. Kubiak, Bull. Chem. Soc. Jpn. 73 (5) (2000) 1205–1212.
[9] I. Tasuko, T. Hamaguchi, H. Nagino, T. Yamaguchi, H. Kido, I.S. Zavarine, T. Richmond, J. Washington, C.P. Kubiak, J. Am. Chem. Soc. 121 (19) (1999) 4625–4632.
[10] C. Londergan, R. Rocha, M.C. Brown, A.P. Shreve, C.P. Kubiack, J. Am. Chem. Soc. 125 (46) (2003) 13912–13913.
[11] G.A. Neyhart, J.T. Hupp, J.C. Curtis, T.J. Meyer, J. Am. Chem. Soc. 118 (15) (1996) 3724–3729.
[12] Z. Fang, S. Swavey, A. Holder, B. Winkel, K.J. Brewer, Inorg. Chem. Commun. 5 (12) (2002) 1078–1081.
[13] L.M. Vogler, B. Scott, K.J. Brewer, Inorg. Chem. 32 (6) (1993) 898–903.
[14] B. Serli, E. Iengo, T. Gianferrara, E. Zangrando, E. Alessio, Met. Drug. 8 (1) (2001) 9–18.
[15] R.L. Williams, N.H. Toft, B. Winkel, K.J. Brewer, Inorg. Chem. 42 (14) (2003) 4394–4400.
[16] M.G. Sauaia, R.G. de Lima, A.C. Tedesco, R.S. da Silva, J. Am. Chem. Soc. 125 (2003) 14718–14719.
[17] L. Alvila, T.A. Pakkanen, J. Mol. Cat. 84 (1993) 145–156.
[18] D. Bianchi, M. Bertoli, R. Tassinari, M. Ricci, M. Vignola, J. Mol. Cat. A: Chem. 200 (1–2) (2003) 111–116.
[19] C. Dragonetti, M. Pizzotti, D. Roberto, S. Galli, Inog. Chim. Acta 330 (2002) 128.
[20] Z. Otwinowski, W. Minor, in: C.W. Carter Jr., R.M. Sweet (Eds.), Processing of X-ray Diffraction Data Collected in Oscillation Mode, Methods in Enzymology, Volume 276, Macromolecular Crystallography. Part A, Academic Press, New York, 1997, pp. 307–326.
[21] M.C. Burla, M. Camalli, B. Carrozzini, G.L. Cascarano, C. Giacovazzo, G. Polidori, R.J. Spagna, Appl. Cryst. 36 (2003) 1103.
[22] G.M. Sheldrick, SHELXTL Version 6. 12, Bruker Analytical X-ray Systems, Bruker AXS, Inc., Madison, Wisconsin, USA, 2002.
[23] G.M. Sheldrick, SHELXL-97, Program for Crystal Structure Refinement, University of Göttingen, 1997.
[24] L.J. Farrugia, J. Appl. Cryst. 32 (1999) 837.
[25] S. Huzinaga (Ed.), Gaussian Basis Sets for Molecular Calculations, Physical Sciences Data 16, Elsevier, Amsterdam, 1984.
[26] M. Haukka, J. Kiviaho, M. Ahlgrén, T.A. Pakkanen, Organometallics 14 (2) (1995) 825–833.
[27] M. Haukka, P. Hirva, S. Luukkanen, M. Kallinen, M. Ahlgrén, T.A. Pakkanen, Inorg. Chem. 38 (13) (1999) 3182–3189.
[28] J.-D. Lee, L.M. Vrana, E.R. Bullock, K.J. Brewer, Inorg. Chem. 37 (14) (1998) 3575–3580.
[29] L. Oresmaa, M. Haukka, P. Vainiotalo, T.A. Pakkanen, J. Org. Chem. 67 (23) (2002) 8216–8219.
[30] A. Salvini, P. Frediani, D. Rovai, M. Bianchi, F. Piacentti, J. Mol. Cat. 89 (1994) 77–92.
[31] M.A. Moreno, M. Haukka, S. Jaaskelainen, S. Vuoti, J. Pursiainen, T.A Pakkanen, J. Organomet. Chem., doi:10.1016/j.jorganchem.2005.05.016.
[32] K.-I. Tominaga, Y. Sasaki, Chem. Lett. 33 (1) (2004) 14–15.
[33] A. Zsigmond, I. Balatoni, K. Bogar, F. Notheisz ans, F. Joo, J. Catal. 227 (2) (2004) 428–435.
[34] L.A.G. Switz, European Patent Application, Patent No. 1510517 (2005).
[35] R.A. Sanchez-Delgado, M. Medina, F. Lopez-Linares, A. Fuentes, J. Mol. Cat. A: Chem. 116 (1997) 167–177.
[36] M.A. Moreno, M. Haukka, M. Kallinen, P.A. Pakkanen, Submitted for publication.
[37] L.D. Slep, S. Pollack, J.A. Olabe, Inorg. Chem. 38 (19) (1999) 4369–4371.
[38] M.I. Bruce, F.G.A. Stone, J. Chem. Soc. A (1967) 1238–1243.
[39] B.F.G. Johnson, R.D. Johnston, J. Lewis, J. Chem. Soc. A (1969) 792–796.
[40] I. Takei, Y. Nishibayashi, Y. Ishii, Y. Mizobe, S. Uemura, M. Hidai, J. Organomet. Chem. 679 (1) (2003) 32–42.
[41] K. Almeida-Lenero, M. Kranenburg, Y. Guari, P.C.J. Kamer, P.W.N.M. van Leeuwen, S. Sabo-Etienne, B. Chaudret, Inorg. Chem. 42(9) (2003) 2859–2866.
[42] J.K. Law, H. Mellows, D.M. Heinekey, J. Am. Chem. Soc. 124 (6) (2002) 1024–1030.
[43] T.P. Fong, A.J. Lough, R.H. Morris, A. Mezzetti, E. Rocchini, P. Rigo, Inorg. Chem. 13 (1998) 2111–2114.
[44] C. Bianchini, C. Mealli, A. Meli, M. Peruzzini, F. Zanobini, J. Am. Chem. Soc. 110 (1988) 8725–8726.
[45] C.-P. Lau, L. Cheng, J. Mol. Cat. (84) (1993) 39–50.
[46] G. Jia, Z. Lin, C.-P. Lau, Eur. J. Inorg. Chem. (2003) 2551–2562.
[47] W.C. Chan, C.P. Lao, Y.Z. Chen, Y.Q. Fang, S.M. Ng, G. Jia, Organometallics 16 (1997) 34–44.
[48] Y-Z. Chen, W.C. Chan, C.P. Lau, H.S. Chu, H.L. Lee, G. Jia, Organometallics 16 (6) (1997) 1241–1246.
[49] G.I. Childs, A.I. Cooper, T.F. Nolan, M.J. Carrot, M.W. George, M. Poliakoff, J. Am. Chem. Soc. 123 (2001) 6857–6866.